CONTENT

Reference

[1] M. H. Rashid. *Power Electronics – Circuits, Devices, and Applications*, 3rd ed. Pearson. 2003.

[2] Emil Levi. *Power Electronics, Drives and Systems*. Course material. 2014.

[3] Richard Crowder. *Electric Drives and Electromechanical Systems.* Elsevier. 2006.

2. POWER ELECTRONIC CONTROL OF DC MOTOR DRIVES

2.1. Introduction

Electric machines are designed for operation with any load torque that is smaller or equal to the rated value and they will run at more or less a constant speed if they are supplied from a voltage source with rated value. Such an operation takes place at the so-called natural torque-speed characteristic of the machine under rated supply conditions. This holds true for both DC and AC machines. Interestingly, the natural torque-speed characteristics can be modified using electric drives. From the application's perspective, the trend of using electric machines in variable speed manner is on the rise. While some conventional, non-power-electronic speed control methods can achieve the variable speed requirement (such as the resistance-based method), it is well known that variable speed operations with power-electronic converters can achieve a higher efficiency. Additionally, some applications also demand accurate control of the position or torque of the machines.

Control of electrical machines can be performed in an open-loop manner or in a closed loop manner. In vast majority of applications where the speed accuracy requirement is low, it is sufficient to perform speed control only in an open-loop manner. Although in principle there is no need for feedbacks of the electrical and mechanical variables in open-loop drives, some measurements are anyway acquired for protection purposes. The motor control algorithm of the drive is simple and the speed is controlled in steady state only with possibly small but acceptable steady-state errors, if no additional provision to mitigate them in the open-loop drives.

On the other hand, numerous applications such as robotics and machine tools require very precise position control and hence require a category of drives commonly known as servo-drives. These drives must be performed in a closed-loop manner with feedbacks of electrical and mechanical variables, and the structure of the control system can be very complicated. Unique features of servo-drives include precise control of position, speed and/or torque in steady state as well as in transient.

DC motors were widely used by industries in servo application before the widespread of power-electronic technology that enhances the AC motors with high-performance variable speed feature. In general, DC motor's speed control is inherently simpler and less expensive than those of AC drives, but this advantage is offset by its bulkiness and significant wear and tear. Although the trend is towards using AC drives, many DC drives are still being used in industries. Hence, the following content of this chapter emphasizes on the fundamentals of DC machines, selected DC drive topologies, and the basic control. Block diagram of a basic electric drive is shown in Fig. 2.1.

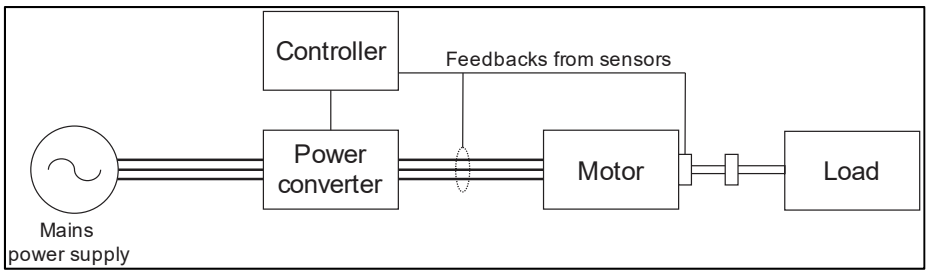

Fig. 2.1: A basic electric drive system consisting an electric source, a power-electronic converter (and auxiliary instrumentation and control components), and a load.

2.2. Fundamentals of DC machines

Armature reaction is a non-ideal phenomenon that is present in a DC motor. Following the Ampere's law, the armature current also creates a magnetic field around the armature winding. This armature field interacts with the field flux and subsequently deviates the magnetic neutral axis from the mid-point between the stator field poles. This has negative consequences such as unaligned commutation which leads electric sparks at the brushes (especially in DC generators) as well as delaying the commutation process. Nevertheless, these issues have been resolved long ago through machine design. Fig. 2.2 shows the internal construction of DC motors and the basic structure of a DC motor.

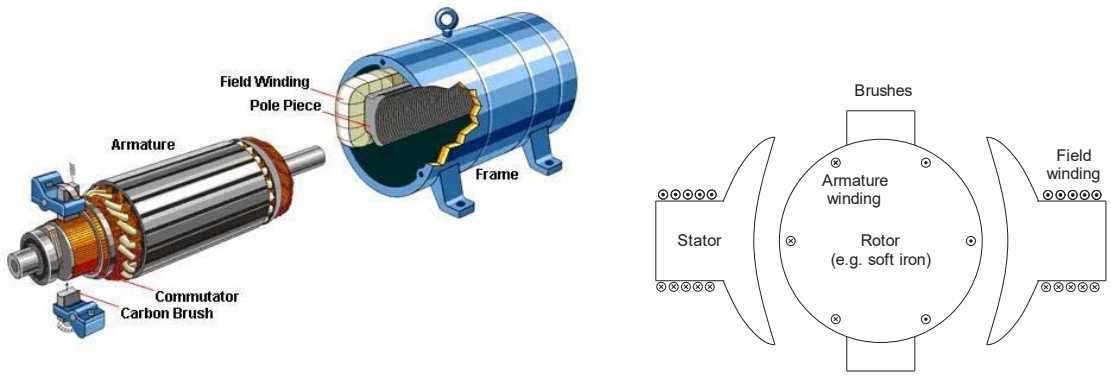

(a) (b)

Fig. 2.2: (a) Graphical illustration of a brushed DC motor (obtained from www.electrical-knowhow.com); (b) basic structure of a DC motor with field and armature windings.

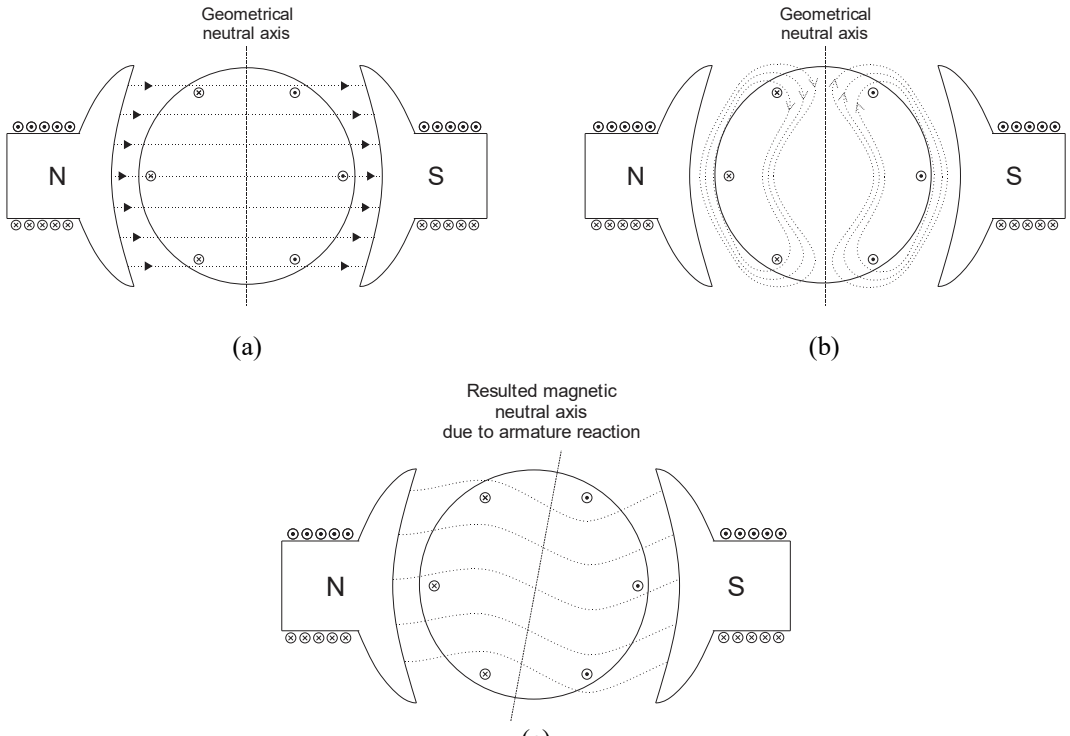

(a) (b)

(c)

Fig. 2.3: (a) Magnetic flux due to field current without the presence of armature flux; (b) magnetic flux due to armature current; (c) Resultant field flux due to armature reaction.

A basic feature of DC motors is the possibility to connect the field and armature windings (assume non-permanent-magnet DC motor) in different ways, as summarized in Fig. 2.4. Each DC motor connection has a slightly different operational characteristics. The emphasis of this chapter, however, is placed on the separately excited DC machines which is the most widely used DC motor in conjunction with electric drives.

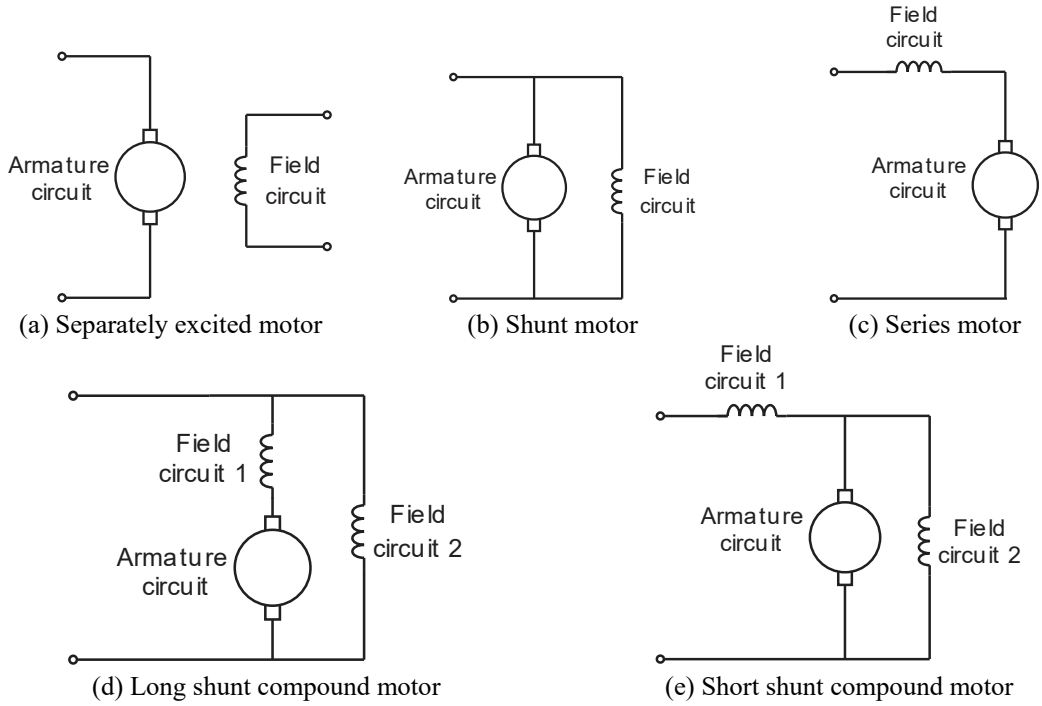

(a) Separately excited motor (b) Shunt motor (c) Series motor

(d) Long shunt compound motor (e) Short shunt compound motor

Fig. 2.4: Variants of DC machines based on the connection of the armature and field windings.

The armature and field windings of a separately excited DC machines are independently excited by separate voltage sources. With supplies that can be controlled to produce the desired armature and field currents, the motor can operate in a wide range speed and with a full range of torque up to its rated value.

DC electric machines can operate in both possible rotational directions (forward or reverse). The direction of rotation is determined by the connection of the DC voltage's polarity. With the advent of power electronic control, the electromagnetic torque of DC machines can be controlled almost instantly (depending on the fastest time constant attainable by the machines subjected to various physical constraints), while the mechanical speed of DC machines is governed by the torque-speed relation. There are four basic operating regions of DC machines, known as forward motoring, forward braking, reverse motoring and reverse braking. They are summarized graphically in Fig. 2.5. Examples of forward motoring and reverse motoring are fans and pumps rotating in forward and reverse direction; an example of forward braking is a forward-moving train going downhill (i.e. the gravitational force is indirectly trying to accelerate the train while the traction drive produces a torque that opposes the external torque to keep the train at a constant speed). These regions are also known as quadrant of operation. A DC drive can operate in single-quadrant (forward or reverse motoring), two-quadrant (e.g. forward-motoring-forward-braking combination in electric vehicle, forward-motoring-reverse-braking combination in crane), or four-quadrant (train) operations, and their implementation requires suitable sets of hardware and control structure.

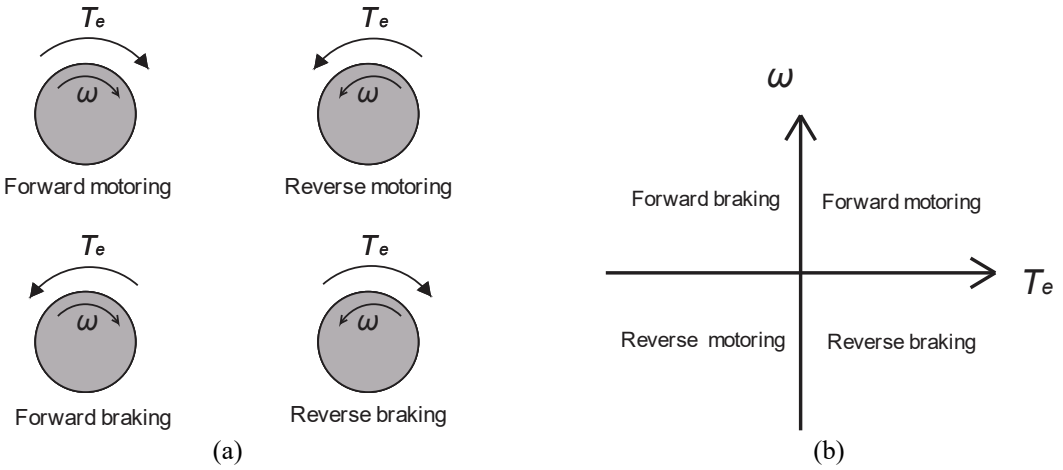

Fig. 2.5: Four-quadrant operation of an electric machine.

Every electric machine has a rated speed value. This value can be understood as the designed speed value at which, given the rated voltage supply, the machine operates at the knee point of the magnetization curve (a.k.a B-H curve) of the saturable iron core, as illustrated in Fig. 2.6 (note that the hysteresis-loop effect and negative ampere-turn/H region are not shown).

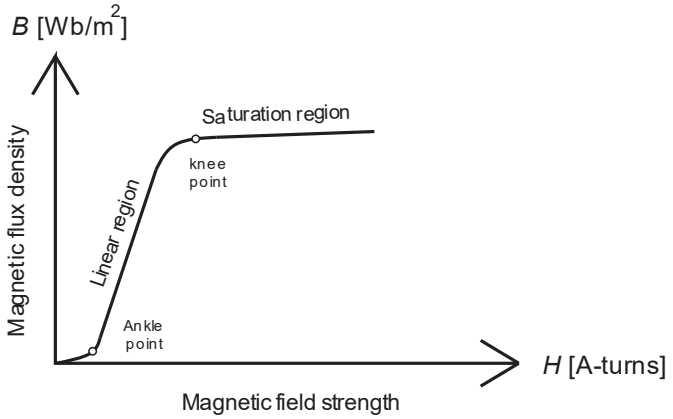

Fig. 2.6: Different regions of a magnetizing curve.

An electrical machine can operate in the speed region below the rated value (until zero, known as the base speed), or the speed region above the rated value (known as the field weakening region, until an absolute maximum speed). In the base speed region, the magnetic flux in the machine is equal to the rated value, and the machine can operate in steady state up to the rated torque. In the field weakening region, the magnetic flux in the machine is reduced by reducing the field current and therefore the magnetic field strength *H*. This also means that the machine no longer operates at the knee point of the magnetizing curve, but a point between the ankle point and knee point.

2.3. Speed control of separately excited DC motors

This section describes the speed-torque characteristic based on the fundamental circuit representation of a separately excited DC motor. The equivalent circuit is shown in Fig. 2.7 below:

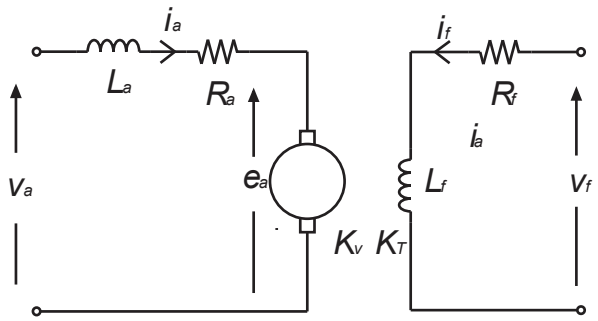

Fig. 2.7: The equivalent circuit of a separately excited DC motor.

The field circuit has the following dynamic voltage balanced equation (note that some references tend to only write the steady-state form):

$$v_f = R_f i_f + L_f \frac{di_f}{dt}$$

where v_f, i_f, R_f and L_f are the terminal voltage across the field winding, current flows in the field, the effective resistance and inductance of the field winding. The armature circuit has the following dynamic voltage balanced equation:

$$v_a = R_a i_a + L_a \frac{di_a}{dt} + e_a$$

where v_a, i_a, R_a and L_a are the terminal voltage across the armature, current flows in the armature, the effective resistance and inductance of the armature winding, and e_a is the back-EMF given by

$$e_a = K_v \omega i_f$$

The electromagnetic torque developed (T_e) by the motor is

$$T_e = K_T i_f i_a$$

where K_v and K_T are the voltage constant and torque constant, whose values (and also R_a and L_a) depend on the physical design of the motor. It is also worth noting that the relationship between the field current i_f and the back EMF e_a is in practice nonlinear due to magnetic saturation. Fig. 2.8 shows a typical no-load voltage (i.e. the back EMF) versus the field current at three different operating speeds.

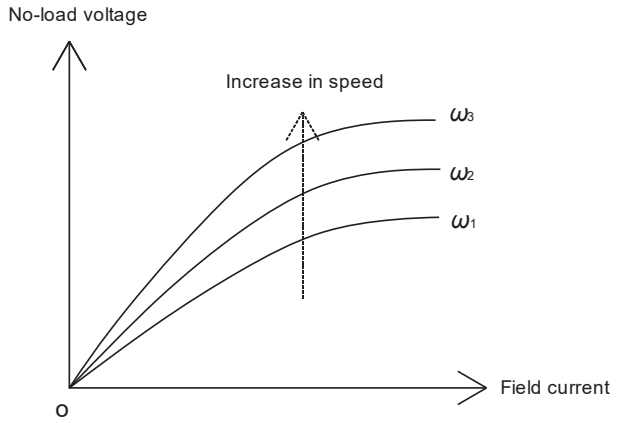

Fig. 2.8: Non-linear relationship between the no-load back EMF and the field current.

Lastly, the basic torque balance equation that governs the speed dynamic:

$$T_e = J\frac{d\omega}{dt} + B\omega + T_L$$

where J, B, and T_L are the total inertia connected to the motor rotor shaft, the viscous friction coefficient and load torque. For analysis purpose or if one only deals with open-loop control, the following can be assumed: given a DC motor under electrical steady state, all time-derivative terms will be nullified:

$$\begin{aligned} V_f &= R_f I_f \\ E_a &= K_v \omega I_f \\ V_a &= R_a I_a + E_a = R_a I_a + K_v \omega I_f \\ T_e &= K_T I_f I_a = B\omega + T_L \end{aligned}$$

Notice that all the small capital voltage and current terms (i.e. instantaneous values) have now been replaced by block capitals, which represent steady-state values. The developed power is calculated from:

$$P_{developed} = T_e \omega$$

The speed of the separately-excited DC motor upon electrical steady state is calculated from:

$$\omega = \frac{V_a - R_a I_a}{K_v V_f / R_f}$$

Given a constant armature/terminal supply voltage in a separately-excited DC motor, T_e is directly proportional to I_a. Exerting an additional load onto a DC machine under steady state will lower the motor speed ω, but the armature current I_a will subsequently be increased (as suggested also by the equation) and this leads to higher electromagnetic torque production. The torque will increase until it counterbalances the additional load to reach a new torque equilibrium. This behavior is reflected clearly by the motor's natural torque-speed characteristics in Fig. 2.9. Note that the plot can either be speed-vs-torque or torque-vs-speed. In this case, it is the former.

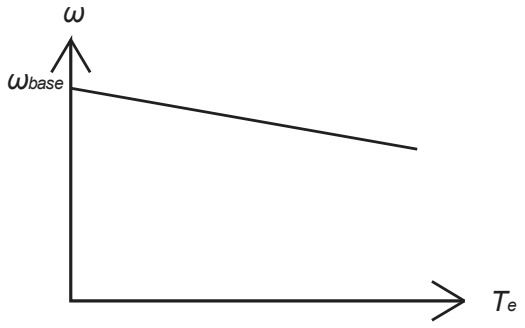

Fig. 2.9: Torque-speed characteristic of a separately excited DC motor.

ω expression above clearly shows that the motor speed can be varied by controlling V_a, I_f, and R_a. Varying R_a (i.e. by connecting a variable resistor in series to the armature winding) is a conventional speed-control method which results in much higher copper losses and is therefore not considered further here. In modern drives with power electronic control, the speed

regulation can be achieved by adjusting V_a or I_f. Speed-torque curves for both types of speed control are summarized in Fig. 2.10.

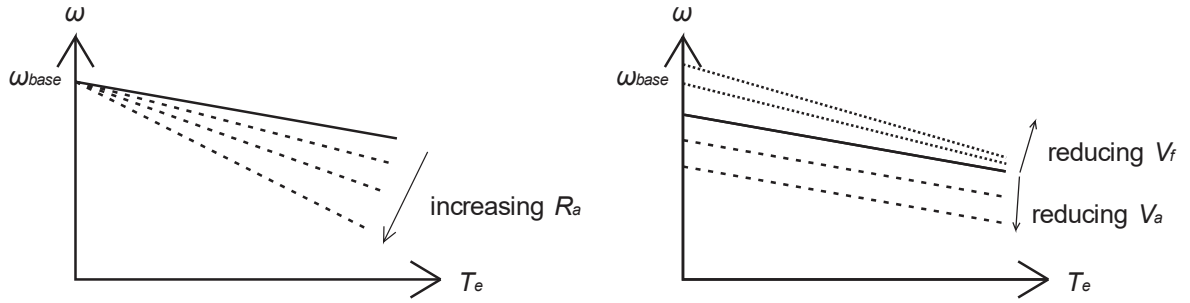

Fig. 2.10: (a) Effects of (a) increasing R_a and (b) reducing V_a and V_f (hence I_f) on the separately excited DC motor's torque-speed characteristics.

Another parameter to be defined is the speed regulation of a DC motor, which is:

$$\text{speed regulation} = \frac{\omega_{no-load} - \omega_{full-load}}{\omega_{full-load}} \times 100\%$$

Fig. 2.11 shows the limits of the torque and power of DC motors under the V_a and I_f control. In the base speed region, V_a control is the dominant technique as the I_f is usually kept at the rated value to produce a rated flux in the DC machines and maximizes the torque production. In the field-weakening region, I_f is reduced as the operating speed increases. V_a is usually kept at the maximum value available to maximize the torque production.

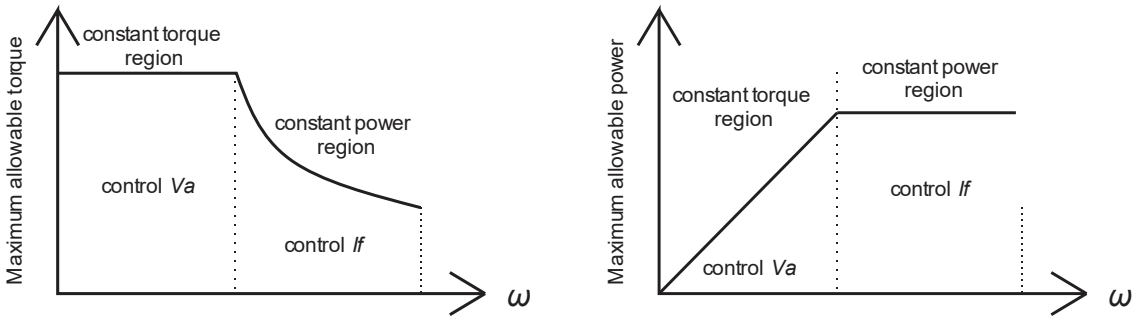

Fig. 2.11: Base speed and field weakening region of an electric machine. (a) The maximum allowable torque and (b) the maximum allowable power of the separately excited DC motor under V_a and I_f control.

2.4. Rectifier Control of separately excited DC motors

The previous section illustrates the principle of speed control in a DC motor. This section describes two methods on how the speed control can be realized. In general, a DC drive can be supplied from a single-phase of a three-phase voltage supply depending on the power requirement. This section of materials requires the understanding the working principle of a controllable bridge rectifier based on thyristors.

Depending on the application requirements such as the quadrants required, one can choose from a number of rectifier-based topologies, e.g. half-wave-converter, full-wave-converter, and etc. as the actuator for speed control of DC motors. The emphasis of this section is placed on a controllable dual-converter drive suppling a separately excited DC motor, as shown in Fig. 2.12. The armature winding is supplied by a controllable three-phase rectifier

and the field winding is supplied by a controllable single-phase rectifier. In this case, all the power electronic switches in the controllable rectifiers are thyristors. This is a two-quadrant drive with forward-motoring and forward-braking operations since the field current is irreversible. The armature current, on the other hand, can be reversed momentarily and this will be described later.

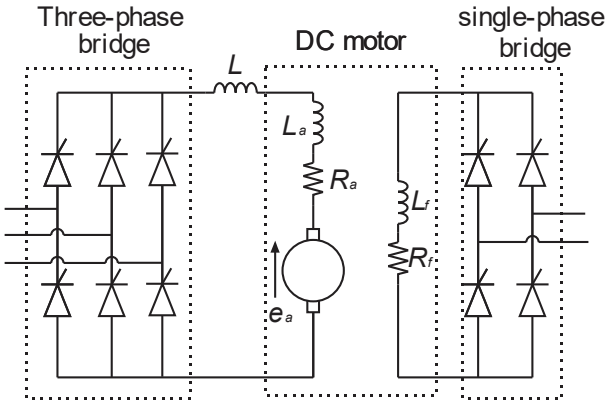

Fig. 2.12: A DC motor drive based on a three-phase fully controllable bridge at the armature winding and a single-phase controllable bridge at the field winding.

Under light loads the torque and hence the armature current required by the machine are small. The instantaneous armature current tends to become discontinuous, which is undesirable because rectifier control assumes continuity of the armature current. Therefore, if the motor's inductance is insufficiently large (which is typical), it is common to add an external inductance L between the rectifier output and the armature for the purpose of improving the current's continuity.

The line-to-neutral/phase voltages and line-to-line/line voltages of a standard three-phase supply are defined as:

$$v_{an} = V_{pk}\sin(\omega t) \qquad v_{ab} = v_{an} - v_{bn} = \sqrt{3}V_{pk}\sin(\omega t + \pi/6)$$
$$v_{bn} = V_{pk}\sin(\omega t - 2\pi/3) \quad \text{and} \quad v_{bn} = v_{bn} - v_{cn} = \sqrt{3}V_{pk}\sin(\omega t - \pi/2)$$
$$v_{cn} = V_{pk}\sin(\omega t + 2\pi/3) \qquad v_{cn} = v_{cn} - v_{an} = \sqrt{3}V_{pk}\sin(\omega t + \pi/2)$$

Then, the average output voltage of the three-phase fully-controllable bridge rectifier in the armature circuit is:

$$V_a = \frac{1}{2\pi}\int_{\frac{\pi}{6}+\alpha_a}^{2\pi+\frac{\pi}{6}+\alpha_a} \sqrt{3}V_{pk}\sin(\omega t+\pi/6)\cdot d(\omega t)$$

$$= 6\left(\frac{1}{2\pi}\int_{\frac{\pi}{6}+\alpha_a}^{\frac{\pi}{2}+\alpha_a} \sqrt{3}V_{pk}\sin(\omega t+\pi/6)\cdot d(\omega t)\right)$$

$$= \frac{3\sqrt{3}V_{pk}}{\pi}\left[-\cos(\omega t+\pi/6)\right]_{\frac{\pi}{6}+\alpha_a}^{\frac{\pi}{2}+\alpha_a}$$

$$= \frac{3\sqrt{3}V_{pk}}{\pi}\left[-\cos(\frac{2\pi}{3}+\alpha_a)+\cos(\frac{\pi}{3}+\alpha_a)\right]$$

$$= \frac{3\sqrt{3}V_{pk}}{\pi}\left[-\cos(\frac{2\pi}{3})\cos\alpha_a+\sin(\frac{2\pi}{3})\sin\alpha_a+\cos(\frac{\pi}{3})\cos\alpha_a-\sin(\frac{\pi}{3})\sin\alpha_a\right]$$

$$= \frac{3\sqrt{3}V_{pk}}{\pi}\cos\alpha_a$$

where $0 < \alpha_a < \pi$ rad, measured from $\pi/3$ rad point from the zero crossing of line voltage V_{ab}, as indicated in Fig. 2.13. V_{pk} is the amplitude of the phase voltage and therefore $\sqrt{3}V_{pk}$ is the amplitude of the line-to-line voltage. By inspection, it can be noticed that the maximum positive average output voltage occurs when $\alpha_a = 0$.

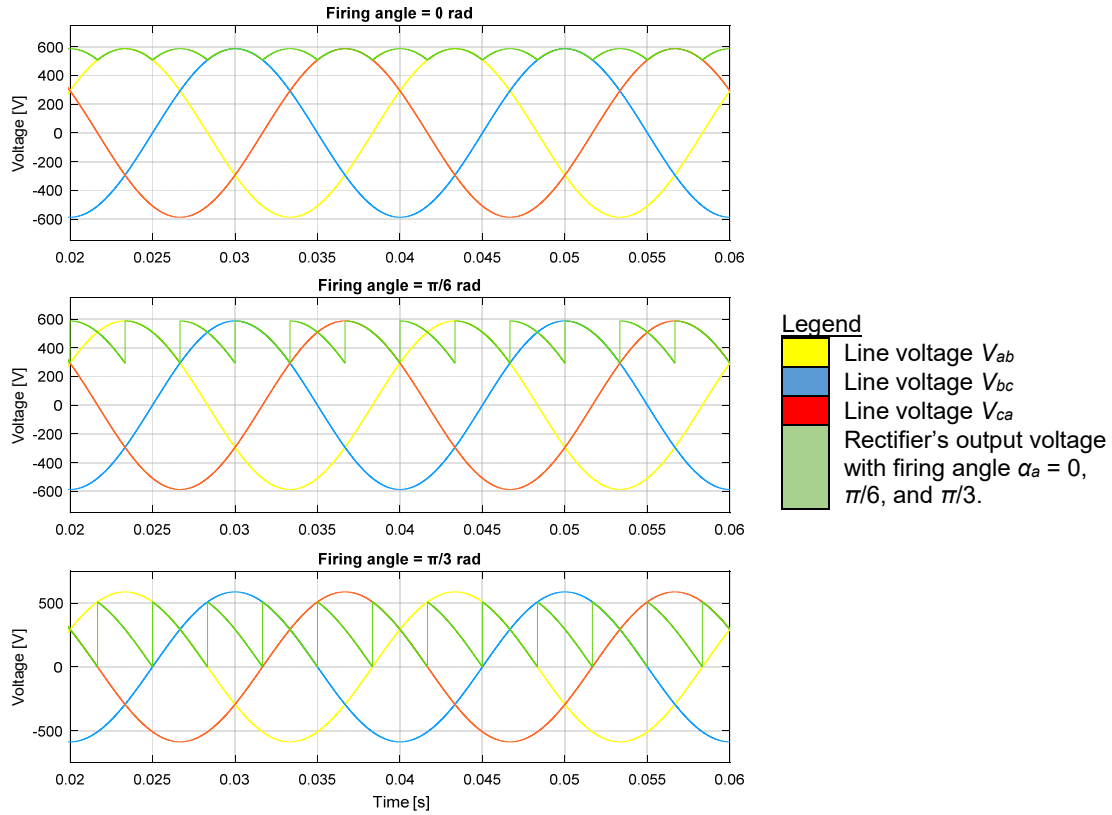

Fig. 2.13: Three-phase and rectifier output voltage waveforms with (middle) firing angle $\alpha_a = \pi/6$ rad and (bottom) firing angle $\alpha_a = \pi/3$ rad.

The rectifier DC output voltage (i.e. the terminal voltage of the armature winding) and hence the armature current contains significant six-order harmonics, as illustrated in Fig. 2.13.

Similar, with the single-phase full converter in the field circuit, the field voltage can be controlled by:

$$V_f = \frac{2V_{pk}}{\pi}\cos\alpha_f$$

For a highly inductive load (such as this case with the large inductance L) where the armature current does not rise/fall across zero within the 50Hz period, the full α can be utilized: for $0 \leq \alpha < \pi/2$ rad, the average output voltage is positive; for $\pi/2 \leq \alpha < \pi$ rad, the average output voltage is effectively negative (but the current is anyway positive, conducted through the anti-parallel diodes. Recall also that thyristors can only conduct unidirectional currents). This mode of operation is known as "inversion" mode. Therefore, a negative terminal voltage with a positive terminal current signifies a regeneration of power from the motor to the AC source. Fig. 2.14 illustrates the inversion mode described above. Fig. 2.15 shows the average output voltage for a fully controllable three-phase bridge rectifier.

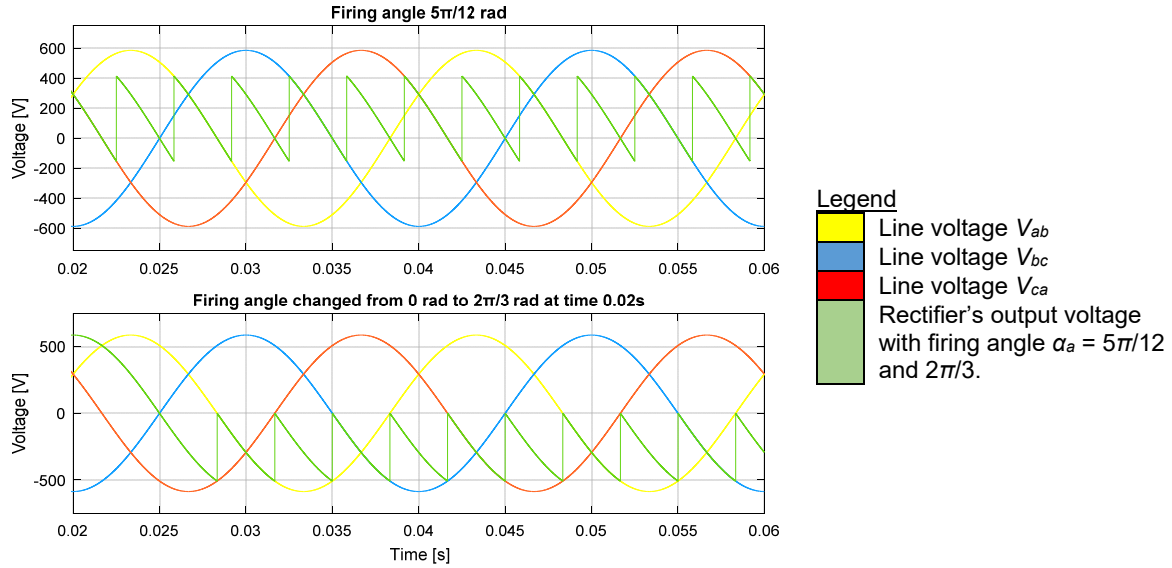

Fig. 2.14: Rectifier output voltage waveforms with large inductance at the output.

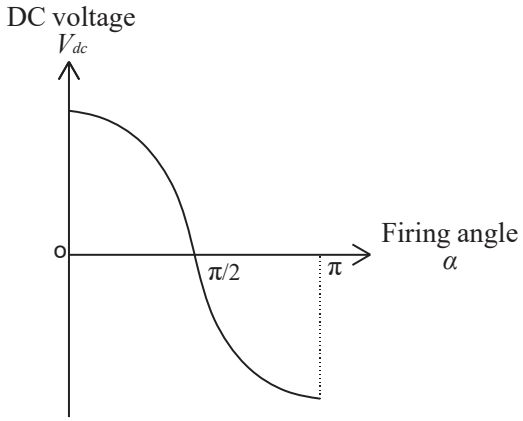

Fig. 2.15: Average output voltage versus the firing angle of the thyristors. The inversion mode is only possible with large output inductance. Otherwise, the voltage will be zero for $\pi/2 < \alpha_a < \pi$.

Lastly, it may be of interest to know the rms value instead of the average value of the output voltage:

$$V = \sqrt{\frac{6}{2\pi}\int_{\frac{\pi}{6}+\alpha_a}^{\frac{\pi}{2}+\alpha_a} 3V_{pk}^2 \sin^2(\omega t + \pi/6)\cdot d(\omega t)}$$

$$= \sqrt{3}V_{pk}\sqrt{\frac{1}{2}+\frac{3\sqrt{3}}{4\pi}\cos 2\alpha_a}$$

2.5. Chopper control of DC machines

In rectifier fed DC drives based on thyristors, the firing angle and hence then armature voltage can be altered only twice in a cycle of the input voltage (i.e. 10 ms for 50Hz AC supply). This limits the achievable dynamic response. Moreover, the machine losses become higher due to the presence of significant low order harmonics in the armature voltage and current waveforms.

Although thyristor-operated chopper is also available, but DC chopper commonly refers to the power electronic converter with PWM-operated switches such as MOSFET or IGBT. The simplest form of chopper with single switch is the single-quadrant DC drive shown in Fig. 2.16.

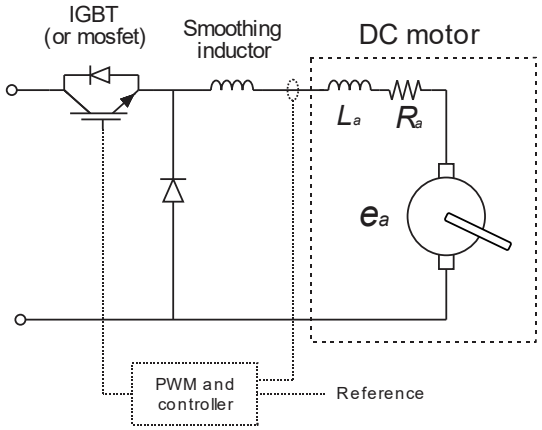

Fig. 2.16: A basic chopper control for illustration purposes.

Nevertheless, this section aims to present a four-quadrant DC drive in conjunction with chopper control, in order to complement the two-quadrant operation described in the earlier section. Fig. 2.17 shows a full H-bridge supplied DC motor drive, which is also known as a four-quadrant DC chopper. A four-quadrant DC chopper can control the load voltage to be positive or negative, and allow bidirectional current flow. Therefore, this topology can control the power flow and the motor speed in the forward direction (voltage positive and current positive), forward regenerative braking (voltage positive; current negative/reverse), reverse direction (voltage negative; current reverse/negative), and reverse regenerative braking (voltage negative; current reverse/positive).

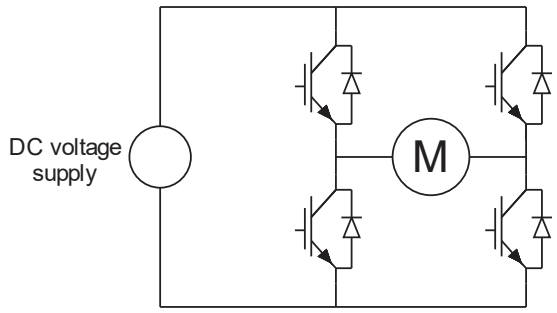

Fig. 2.17: A full H-bridge based chopper control of a DC motor.

Refer to Fig. 2.17, the input DC voltage can be supplied from a smoothened diode-rectified AC voltage (single-phase or three-phase, depending on the power requirement), a active rectifier output, or simply from a DC voltage source such as battery or DC overhead line.

The four IGBT switches form an H-bridge that is controlled by pulse width modulation (PWM). Standard PWM has constant switching frequency F_s and therefore constant switching period is $T_s = 1/F_s$. The state-of-the-art PWM technique for H-bridges is the bipolar voltage switching method. As the name suggests, both legs of the H-bridge will be used in each switching period. The PWM operation is illustrated in Fig. 2.18.

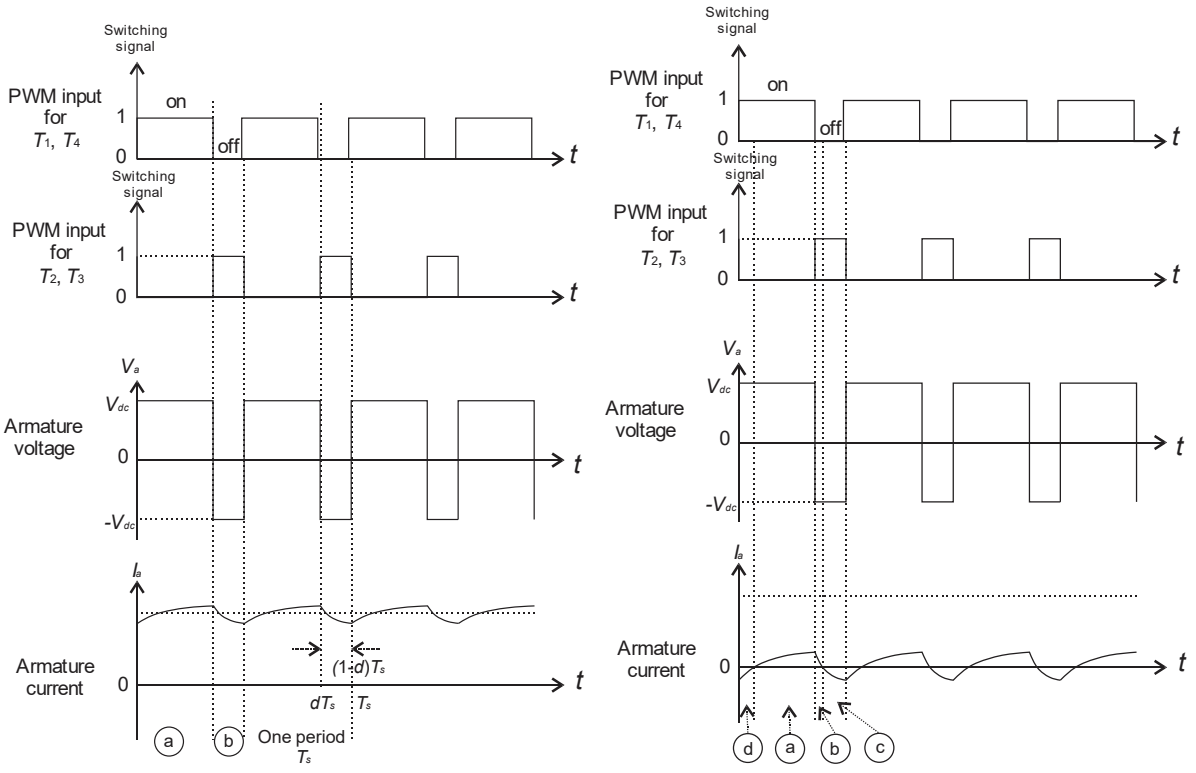

Fig. 2.18: Voltage and current waveforms during the (left, a) continuous conduction mode; (right, b) discontinuous conduction mode.

The four switches can be grouped into two groups: T_1 and T_4; T_2 and T_3. Both switches in each pair are meant to be turned on/off simultaneously and the two pairs are to be operated in the complementary manner. In order to simply the following analysis, the switches are assumed to have insignificant internal voltage drop and no dead time is inserted. Dead time is

a blanking time during which both switches (in an H-bridge leg) are turned out to prevent shoot through, i.e. short-circuiting the DC bus. In practice, depending on the voltage and power levels of the power-electronic switches, dead-time of 2-8ms are normally inserted at each switch toggling.

Depending on the magnitude of armature current and switching frequency, the H-bridge can be in the discontinuous conduction mode or continuous conduction mode. In the continuous conduction mode, within each of the switching period, there are two operational sub-cycles (Fig. 2.18a):

(a) T_1 and T_4 are turned on, and the armature current flows in the positive direction;
(b) T_2 and T_3 are turned on but not conducting. Instead, freewheeling diodes D_2 and D_3 are latched on, and the armature current flows in the positive direction;

The same applies to negative armature current. In the discontinuous conduction mode, within each of the switching period, there are four operational sub-cycles (Fig. 2.18b):

(c) T_1 and T_4 are turned on, and the armature current flows in the positive direction;
(d) T_2 and T_3 are turned on but not conducting. Instead, freewheeling diodes D_2 and D_3 are latched on, and the armature current flows in the positive direction;
(e) T_2 and T_3 are turned on and conducting, and the armature flows in the negative direction;
(f) T_1 and T_4 are turned on but not conducting. Instead, freewheeling diodes D_1 and D_4 are latched on, and the armature current flows in the negative direction;

The effective voltage and current values can be calculated from first principle, i.e. based on the basic circuit theory. Depending on the design requirement such as the situation when the switching frequency shall not exceed a certain value, further reduction of current ripple can be based on the addition of external series inductor in series with the motor and this will then affect the effective voltage and current calculation.

Assume that upon steady state, the instantaneous current in the motor is I_1 in the beginning of each switching period. When T_1 and T_4 are ON and the current flows in the positive direction through the RL, the back-EMF E, the switches T_1 and T_4, and the source V_{dc}:

$$V_{dc} = L\frac{di}{dt} + Ri + E$$

Given the initial instantaneous current of I_1 and for $0 < t < kT$, the exact solution for this differential equation is:

$$i_1(t) = I_1 e^{-\frac{R}{L}t} - \frac{(E - V_{dc})}{R}\left[1 - e^{-\frac{R}{L}t}\right]$$

The current will rise to I_2 and the end of ON period of T_1 and T_4. This is reflected by substituting $t = kT$ and $i_1 = I_2$ to get the relationship of:

$$I_2 = I_1 e^{-\frac{R}{L}kT} - \frac{(E - V_{dc})}{R}\left[1 - e^{-\frac{R}{L}kT}\right]$$

When T_2 and T_3 are ON and the current continues to folow in the positive direction through the RL, the back-EMF E, the anti-parallel diodes of T_2 and T_3, and the source V_{dc}:

$$-V_{dc} = L\frac{di}{dt} + Ri + E$$

Given the initial instantaneous current I_2 and for $0 < t < (1\text{-}k)T$, the exact solution for this differential equation is:

$$i_2(t) = I_2 e^{-\frac{R}{L}t} - \frac{(E+V_{dc})}{R}\left[1 - e^{-\frac{R}{L}t}\right]$$

In the case of continuous-current scenario, the current will fall to I_2 and the end of ON period of T_2 and T_3. This is reflected by substituting $t = (1\text{-}k)T$ and $i = I_1$ to get the relationship of:

$$I_1 = I_2 e^{-\frac{R}{L}(1-k)T} - \frac{(E+V_{dc})}{R}\left[1 - e^{-\frac{R}{L}(1-k)T}\right]$$

Lastly, solve the simultaneous equations to get I_1 and I_2 in terms of circuit parameters, the switching period T, and duty cycle k:

$$I_1 = -\frac{E}{R} + \frac{V_{dc}}{R}\left[\frac{2e^{-\frac{R}{L}(1-k)T} - e^{-\frac{R}{L}T} - 1}{1 - e^{-\frac{R}{L}T}}\right]$$

$$I_2 = -\frac{E}{R} + \frac{V_{dc}}{R}\left[\frac{-2e^{-\frac{R}{L}kT} + e^{-\frac{R}{L}T} + 1}{1 - e^{-\frac{R}{L}T}}\right]$$

Upon steady state, the average voltage and current across/through the load are calculated from:

$$\langle V \rangle = \frac{1}{T}\left[\int_0^{kT} V_{dc} \cdot dt + \int_{kT}^{(1-k)T} -V_{dc} \cdot dt\right] = (2k-1)V_{dc}$$

$$\langle i \rangle = \frac{1}{T}\left[\int_0^{kT}\left\{I_1 e^{-\frac{R}{L}t} - \frac{(E-V_{dc})}{R}\left(1 - e^{-\frac{R}{L}t}\right)\right\}.dt + \int_0^{(1-k)T}\left\{I_2 e^{-\frac{R}{L}t} - \frac{(E+V_{dc})}{R}\left(1 - e^{-\frac{R}{L}t}\right)\right\}.dt\right]$$

2.6. Regenerative braking

In order to realize generative braking, an active current control at the voltage terminal is assumed, as depicted by Fig. 2.19.

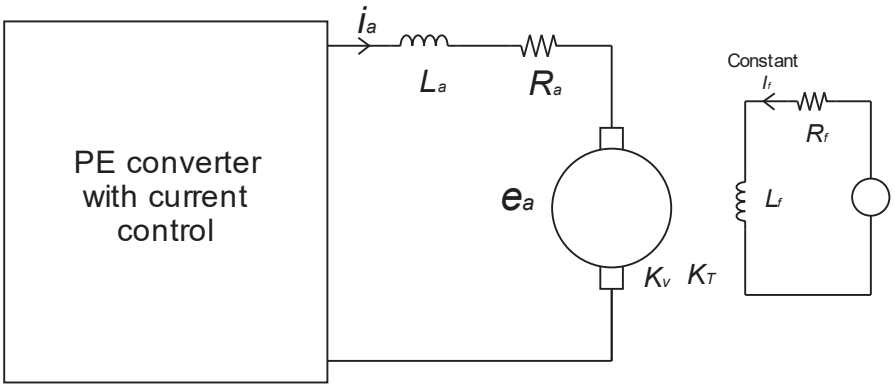

Fig. 2.19: Regenerative braking of a DC motor.

The generalized DC motor's voltage balanced equation and the DC motor torque are:

$$v_m = K_e\omega_m + i_a R_a + L_a \frac{di_a}{dt}$$

$$T = K_t i_a$$

$$T = J\frac{d\omega_m}{dt} + B\omega_m$$

where ω_m is the speed of rotation, in rad/s; K_e is the motor's speed constant, in V/(rad/s); K_t is the motor torque constant, in Nm/A; L_a is the armature inductance, in H; and T is the electromagnetic torque, in Nm. Field current is assumed to be constant and therefore has been accounted for by K_e and K_t. Copper loss at the armature is:

$$P_d = i_a^2 R_a$$

The braking current is controlled by the DC drive to remain constant I_R (negative) during the braking period, the voltage balanced equation can then be simplified to:

$$V_m(t) = K_e\omega_m(t) + I_a R_a + 0$$

Assume that the windage friction is zero, no load is connected, and with constant braking armature current, the braking torque therefore remain constant too during the braking period. The deceleration is therefore a constant and the speed profile is a straight line (Fig. 2.20):

$$\omega_m(t) = \left(1 - \frac{t}{t_z}\right)\omega_{\text{int}}$$

where the starting instant of braking is assumed to be at t =0, i.e.

$$\omega_{\text{int}} = \omega_m(0)$$

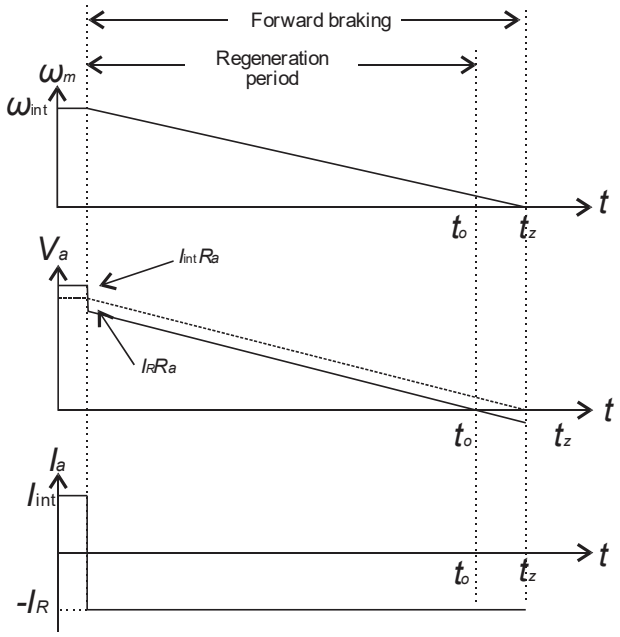

Fig. 2.20: Evolution of terminal voltage and current (i.e. braking currents) with respect to the changes of motor speed throughout the braking period.

Prior to deceleration from ω_{int}, the terminal voltage is equal to ($K_e\omega_{\text{int}} + I_{\text{int}}R_a$, where I_{int} is positive). Immediately following the application of the negative braking current the terminal voltage drops to ($K_e\omega_{\text{int}} + I_R R_a$, where I_R is negative). $K_e\omega_{\text{int}}$ is the initial back EMF. V_m decreases as the speed ω_m decreases due to decreasing back EMF until it crosses zero. This happens when $K_e\omega_m(t) = I_R R_a$ at $t = t_o$. The motor will continue decelerating until reaching standstill $\omega_m(t) = 0$ at $t = t_z$. The motor's terminal voltage during the deceleration can be written as:

$$V_m(t) = K_e\left(1 - \frac{t}{t_z}\right)\omega_{\text{int}} + I_R R_a$$

$$V_m(t) = -\frac{K_e\omega_{\text{int}}t}{t_z} + K_e\omega_{\text{int}} + I_R R_a$$

The time t_o can be determined by equating the terminal voltage to zero, giving:

$$0 = -\frac{K_e\omega_{\text{int}}}{t_z}t_o + K_e\omega_{\text{int}} + I_R R_a$$

Solve for t_o:

$$t_o = t_z\left(1 + \frac{I_R R_a}{K_e\omega_{\text{int}}}\right)$$

Recall that that I_R has a negative value during the regeneration (during $0 \leq t \leq t_z$). The regenerative power obtainable is defined as:

$$P_{regen} = V_m(t)I_R$$

Although the braking happens from $t = 0$ to $t = t_z$, the regeneration period is spanned from $t = 0$ to $t = t_o$. From $t = t_o$ to $t = t_z$, both the terminal voltage and braking current are negative,

suggesting energy consumption in the motor. Hence the regenerated energy during this period is:

$$\begin{aligned} E_{regen} &= \int_0^{t_o} V_m(t) I_R \cdot dt \\ &= \int_0^{t_o} \left[-\frac{K_e \omega_{\text{int}} t}{t_z} + K_e \omega_{\text{int}} + I_R R_a \right] I_R \cdot dt \\ &= t_o \left[\frac{K_e \omega_{\text{int}} I_R}{2} + \frac{I_R^2 R_a}{2} \right] \end{aligned}$$

Braking torque developed during the deceleration/regeneration (assume no load and no windage friction):

$$T_{braking} = K_t I_R = J\alpha$$

$$\alpha = \frac{K_t I_R}{J}$$

Given the deceleration required (care with the sign) is $\alpha = \frac{0 - \omega_{\text{int}}}{t_z}$, then:

$$\frac{K_t I_R}{J} = \frac{-\omega_{\text{int}}}{t_z}$$

$$t_z = \frac{-J\omega_{\text{int}}}{K_t I_R}$$

From the relationship between t_o and t_z:

$$t_o = \frac{-J\omega_{\text{int}}}{K_t I_R} \left(1 + \frac{I_R R_a}{K_e \omega_{\text{int}}} \right)$$

Then, the calculated regenerated energy from $t = 0$ to $t = t_o$ can also be expressed as:

$$\begin{aligned} E_{regen} &= t_o \left[\frac{K_e \omega_{\text{int}} I_R}{2} + \frac{I_R^2 R_a}{2} \right] \\ &= \frac{-J\omega_{\text{int}}}{K_t I_R} \left(1 + \frac{I_R R_a}{K_e \omega_{\text{int}}} \right) \left[\frac{K_e \omega_{\text{int}} I_R}{2} + \frac{I_R^2 R_a}{2} \right] \\ &= \frac{-J\omega_{\text{int}}}{K_t} \left[\frac{K_e \omega_{\text{int}}}{2} + \frac{I_R^2 R_a^2}{2 K_e \omega_{\text{int}}} + I_R R_a \right] \end{aligned}$$

Recall that this energy expression is based on the assumptions of constant braking current (hence torque), no load torque, and no friction.